

Slug/SNAI2 regulates cell proliferation and invasiveness of metastatic prostate cancer cell lines

Modjtaba Emadi Baygi · Zahra-Soheila Soheili ·
Frank Essmann · Abdolkhaleg Deezagi ·
Rainer Engers · Wolfgang Goering · Wolfgang A. Schulz

Received: 3 December 2009 / Accepted: 2 April 2010 / Published online: 27 May 2010
© International Society of Oncology and BioMarkers (ISOBM) 2010

Abstract Many metastatic cancers recapitulate the epithelial-to-mesenchymal transition (EMT) resulting in enhanced cell motility and invasiveness. The EMT is regulated by several transcription factors, including the zinc finger protein SNAI2, also named Slug, which appears to exert additional functions during development and cancer progression. We have studied the function of SNAI2 in prostate cancer cells. Quantitative RT-PCR analysis showed strong *SNAI2* expression particularly in the PC-3 and PC3-16 prostate carcinoma cell lines. Knockdown of SNAI2 by specific siRNA induced changes in EMT

markers and inhibited invasion of both cell lines into a matrigel matrix. SNAI2 siRNA-treated cells did not tolerate detachment from the culture plates, likely at least in part due to downregulation of integrin $\alpha 6\beta 4$. SNAI2 knockdown disturbed the microtubular and actin cytoskeletons, especially severely in PC-3 cells, resulting in grossly enlarged, flattened, and sometimes multinuclear cells. Knockdown also decreased cell proliferation, with a prominent G0/G1 arrest in PC3-16. Together, our data imply that SNAI2 exerts strong effects on the cytoskeleton and adhesion of those prostate cancer cells that express it and is necessary for their proliferation and invasiveness.

Electronic supplementary material The online version of this article (doi:10.1007/s13277-010-0037-5) contains supplementary material, which is available to authorized users.

M. Emadi Baygi
Department of Genetics, Faculty of Basic Sciences,
Tarbiat Modares University,
Tehran, Iran

Z.-S. Soheili · A. Deezagi
Department of Biochemistry, National Institute
of Genetic Engineering and Biotechnology,
Tehran, Iran

F. Essmann
Interfaculty Institute of Biochemistry, Eberhard Karls University,
Tübingen, Germany

R. Engers
Institute of Pathology, Heinrich Heine University,
Moorenstrasse 5,
40225 Düsseldorf, Germany

W. Goering · W. A. Schulz (✉)
Department of Urology, Heinrich Heine University,
P. O. Box 40225, Düsseldorf, Germany
e-mail: wolfgang.schulz@uni-dusseldorf.de

Keywords Slug · Cell cycle arrest · Cell shape ·
Invasiveness · Integrin $\alpha 6\beta 4$ · Cytoskeleton ·
Epithelial–mesenchymal transition

Introduction

Prostate cancer (PCa) is a major health problem in Western industrialized countries. Since there is currently no curative treatment for metastatic disease, the decisive factor for its outcome is the ability of cancer cells to metastasize to other tissues. Many metastatic cancers appear to recapitulate a normal developmental process, the epithelial-to-mesenchymal transition (EMT), which is associated with enhanced cell motility and invasiveness [1]. EMT is regulated by several transcription factors, such as Snail (SNAI1), Slug (SNAI2), Twist, E47, and ZEB. They increase the expression of mesenchymal markers, such as N-cadherin and vimentin, and concomitantly repress proteins essential for establishment of cell–cell adhesion and epithelial morphology like E-cadherin and cytokeratins [2].

SNAI2 is a member of the Snail super family of zinc finger transcription factors [1] that recognize E-box consensus binding sites with the core sequence CANNTG [3]. Although increased *SNAI2* expression has been linked to the aggressiveness of several cancer types [4], the biological processes influenced by the factor and the molecular mechanisms involved have not been precisely elucidated [5]. Overexpression of either SNAI2 or SNAI1 is sufficient to induce EMT in cultured epithelial cells [6]. In breast cancers, expression of SNAI2 was shown to correlate with loss of E-cadherin transcripts [7], to cause desmosome dissociation [8], and to regulate negatively the expression of cytokeratins 8 and 19 [9]. In addition to its role in EMT, overexpressed SNAI2 could affect tumor cell fate after treatment with genotoxic agents [10] and has been proposed to confer resistance to cell death induced by inherent genetic instability [11].

Since to date, SNAI2 function in prostate cancer has not been characterized, we used siRNA-mediated downregulation (knockdown) to analyze the role of SNAI2 in EMT and other suggested SNAI2-associated functions in prostate carcinoma cell lines. As we observed that *SNAI2* expression was largely restricted to PC-3 and its sublines, we investigated PC-3 and its derivative PC3-16, which has been isolated from a lymph node metastasis of a PC-3 orthotopic implant and displays a more mesenchymal phenotype [12] and a particularly high expression of *SNAI2*. Our results show for the first time that SNAI2 exerts unexpectedly diverse functions in certain prostate cancer cells beyond the regulation of EMT.

Methods and materials

Cell lines and cell cultivation procedures

The prostate carcinoma cell lines LNCaP, PC-3 and its two derivatives PC3-16 and PC3-24, 22Rv1, and DU145 were cultured in RPMI-1640 (Gibco Life Technologies, Karlsruhe, Germany), supplemented with 10% fetal calf serum and 100 U/ml penicillin/10 µg streptomycin. The PC-3 derivatives [12] were kindly provided by Dr. V. Jung, Medical University of the Saarland. PC3-16 is a subline derived from a lymph node metastasis of this orthotopically implanted line. PC3-24 was derived from a lung metastasis. MDA-PCa2b was cultured as described [13]. Normal prostate epithelial cells purchased from Cambrex (Verviers, Belgium) were cultured as recommended by the supplier.

RNA interference

Double-stranded, short (21-mer) interfering RNA (siRNA) corresponding to *SNAI2* mRNA and an irrelevant siRNA

with the following sense and antisense sequences were purchased from MWG (Ebersberg, Germany):

Slug/SNAI2: (sense; antisense)

CGAACUCAGGUGCCUUAAdTdT; UUUAAGGC
ACCUGAGUUCGdCdG

Irrelevant [14]: (sense; antisense)

CUGAUGCAGGUAUCGCGUdTdT; ACGCGAAU
ACCUGCAUCAGdTdT

For knockdown experiments, cells were seeded in six-well plates at 1.5×10^5 cells per well. The next day, when the cultures were 30–50% confluent, cells were transfected with 25 (PC-3) or 30 nM (PC3-16) siRNA using Lipofectamine RNAiMAX (Invitrogen, Karlsruhe, Germany). Unless indicated otherwise, all further assays were performed 72 h after transfection.

RNA extraction and analysis

Total RNA was isolated using Qiazol reagent (Qiagen, Hilden, Germany) and RNeasy columns (Qiagen) and was further purified by in-column DNase I digestion (Qiagen). Synthesis of cDNA was performed using SuperScriptII reverse transcriptase (Invitrogen) with oligo-dT and random primers, according to the manufacturer's protocol.

Real-time RT-PCR was performed using a LightCycler II (Roche, Mannheim, Germany). Real-time RT-PCR for Integrin $\alpha 6$ (*ITGA6*), Integrin $\beta 4$ (*ITGB4*), and TATA-box binding protein (*TBP*) mRNAs was performed using specific Quantitect primer assays (Qiagen) with the QuantiTect SYBR Green PCR Kit (Qiagen). Real-time RT-PCR for Slug (*SNAI2*), Snail (*SNAI1*), E-cadherin (*CDH1*), Keratin-18 (*KRT18*), and vimentin (*VIM*) mRNAs was done using specific primers (Table 1) with the LightCycler-FastStart DNA Master PLUS SYBR Green I kit (Roche, Mannheim, Germany). The PCR for the five latter genes included an initial denaturation step at 95°C for 10 min, followed by 45 amplification cycles consisting of denaturation at 95°C for 10 s, annealing at 60°C for 10 s, and extension at 72°C for 10 s. All measurements were performed in at least duplicates; variance was less than 10%.

Assays for cellular effects

Cell viability was determined by the Cell Titer-Glo Luminescent Cell Viability Assay (Promega, Mannheim, Germany) according to the manufacturer's protocol. Staining for senescence-associated β -galactosidase was done according to a previously published protocol [15].

For cell cycle analysis by flow cytometry, cells were harvested, washed with PBS, and stained with 50 µg/ml

Table 1 Sequence of RT-PCR primers

| Designation | Sequence | Product size (bp) |
|---------------|---------------------------|-------------------|
| Snail fw | TTGGATACAGCTGCTTTGAG | 150 |
| Snail rv | ATTGCATAGTTAGTCACACCTC | |
| Slug fw | GAGTCTGTAATAGGATTTCCCATAG | 122 |
| Slug rv | CTTTAGTTCAACAATGGCAAC | |
| E-cadherin fw | ACCAGAATAAAGACCAAGTGACCA | 171 |
| E-cadherin rv | AGCAAGAGCAGCAGAATCAGAAT | |
| Keratin-18 fw | ACACAGTCTGCTGAGGTTGGAG | 160 |
| Keratin-18 rv | TGCTCCATCTGTAGGGCGTAG | |
| Vimentin fw | AATGGCTCGTCACCTTCGTGAAT | 159 |
| Vimentin rv | CAGATTAGTTCCCTCAGGTTTCAG | |

propidium iodide solution containing 0.1% triton X-100 and sodium citrate as described [16] and were then analyzed for relative DNA content using a FACSCalibur instrument (Becton Dickinson, Heidelberg, Germany). Profiles were analyzed using CellQuestPro software (Becton Dickinson).

Apoptosis was followed by determination of caspase-3 and caspase-7 activities by the Caspase-Glo 3/7 assay kit (Promega) in a plate reader luminometer (Victor2, Perkin-Elmer) with normalization to cell numbers.

For re-attachment assays, cells were harvested by trypsinization 48 h after the first transfection and then suspended in a bacterial plate. At various intervals, cells were transferred to a new 6-well cell culture plate, allowed to grow until the mock-treated cells became confluent, and Giemsa-stained.

In vitro invasiveness was determined by means of the Matrigel invasion assay, which was essentially performed as described [17].

Western blotting

Cytoplasmic and nuclear proteins from cells were prepared using a commercially available nuclear extraction kit (Active Motif, Carlsbad, CA, USA). The nuclear proteins were resolved on a 12% SDS-PAGE gel (Biorad, Hercules, CA, USA) and electrotransferred onto Immobilon-P membranes (Millipore, Hamburg, Germany). Membranes were blocked for 1 h with 5% milk powder in PBS plus 0.05% tween 20. Samples were then probed successively with rabbit polyclonal antibody against SNAI2 (1:100; Santa Cruz, CA, USA), and monoclonal antibody against TBP (1:1500; Abcam, UK) and subsequently with horseradish peroxidase (HRP)-conjugated anti-rabbit (1:5,000; Santa Cruz) or HRP-conjugated secondary anti-mouse (1:5,000; Santa Cruz) antibodies, respectively. E-Cadherin was investigated in whole cell lysates using a mouse monoclonal antibody (1:5,000, Santa Cruz) and subsequently a goat polyclonal antibody against α -tubulin (1:10,000, Santa Cruz). Bands were visualized

using a chemiluminescence kit (Amersham Biosciences, Freiburg, Germany).

Cell surface staining

Cells (1.5×10^6) were incubated with monoclonal antibody against integrin $\alpha 6$ (1:1,000; Abcam) for 15 min at 4°C, washed with FACS buffer (PBS with 2% BSA), incubated for another 15 min with Alexa Fluor 488 goat anti-mouse IgG (1:1,000; Invitrogen), and after further washing analyzed in a FACSCalibur instrument (Becton Dickinson).

Confocal laser scanning microscopy

Cells were fixed with methanol/acetone (1:1) at -20°C and subsequently incubated for 1 h in phosphate-buffered saline containing 4% bovine serum albumin and 0.05% saponine and then overnight with anti- α -tubulin (DM1a, 1:500, Sigma) and anti- γ -tubulin (1:300; Sigma) antibodies or with anti- α -tubulin and β -actin (1:300; Sigma) antibodies. Thereafter, cells were washed 2 \times in PBS and stained with secondary antibodies (Alexa 488- and Alexa 592-coupled anti-mouse or anti-rabbit IgG, Invitrogen) at 4 $\mu\text{g}/\text{ml}$. DNA was detected using 4,6-diamidino-2-phenylindole (DAPI, 1 mg/ml; Sigma). Analyses were performed with a Leica TCS SP2/AOBS microscope equipped with a HCX PL APO $\times 63$ immersion objective and excitation wavelengths of 405, 488, and 594 nm. Figures shown are projections of recorded z stacks of various dimensions and have a resolution of at least 512×512 pixels.

Statistical analyses

All experiments were repeated at least three times, and statistical significance was measured by the paired Student t test or the nonparametric Mann–Whitney U test (invasion assay). p values of <0.05 were considered to indicate statistical significance.

Results

SNAI2 is expressed in normal prostate epithelial cells and selected carcinoma cell lines

Expression of *SNAI2* was investigated by quantitative RT-PCR in established prostate carcinoma cell lines (Supplementary Table 1) as well as normal prostate epithelial cells (Fig. 1). Of eight carcinoma cell lines, PC3-16 showed the highest expression, and the expression in the parental cell line PC-3 was moderate. In the other carcinoma cell lines, expression was distinctly lower. Intriguingly, normal prostate epithelial cells, which had been harvested at low density, also expressed *SNAI2* mRNA. Based on these results, we selected the PC3-16 and PC-3 cell lines for knockdown experiments.

SNAI2 expression is specifically downregulated by siRNA treatment

Application of *SNAI2*-siRNA resulted in a dramatic reduction in *SNAI2* mRNA expression (up to 90%, $p < 0.05$) compared to IR-siRNA-treated cells, as determined by RT-PCR (Fig. 2a). The siRNA against *SNAI2* did not affect expression of the closely related *SNAI1* gene (Fig. 2b). To assess whether the effect extended to the *SNAI2* protein, we performed western blotting on siRNA-transfected PC-3 cells. As is evident in Fig. 2c, *SNAI2* protein was successfully downregulated by *SNAI2*-specific siRNA in PC3 cells, adjusted to TBP by 63%. Due to high

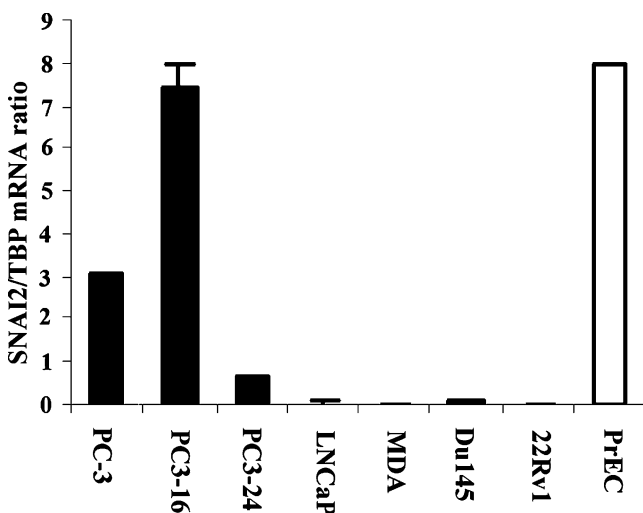


Fig. 1 Expression of *SNAI2* in normal prostate epithelial cells and carcinoma cell lines. Histograms comparing the relative gene expression of *SNAI2* to *TBP* (TATA-box binding protein) as determined by quantitative RT-PCR in normal prostate epithelial cells (white column) and carcinoma cell lines (black columns). Values shown represent the mean \pm SEM

background in repeated experiments, we could not verify the downregulation of *SNAI2* in PC3-16 cells.

Expression of EMT markers changes after siRNA treatment

Next, we investigated the effect of *SNAI2* knockdown on the expression of typical EMT markers such as E-cadherin (*CDH1*), Keratin 18 (*KRT18*), and Vimentin (*VIM*) (Fig. 3). *CDH1* and *KRT18* expression increased in both PC-3 and PC3-16 cell lines following *SNAI2* siRNA treatment (Fig. 3a, b), while *VIM* expression (Fig. 3c) decreased in both cell lines, although not to a statistically significant extent. Of note, E-cadherin mRNA expression in PC3-16 was only about 1% that in PC-3. Accordingly, in PC3-16 cells, E-cadherin protein remained undetectable even after the substantial increase following treatment with Slug siRNA, whereas in PC-3 cells, a slight increase in E-cadherin protein was detectable (Fig. 3d).

Cell viability is reduced after *SNAI2* suppression

The effect of *SNAI2* knockdown on cell proliferation was analyzed by the cell Titer-Glo luminescent cell viability assay kit, which estimates the number of viable cells based on overall ATP amounts. There was a pronounced and significant reduction in the relative luminescence of *SNAI2*-siRNA-treated cells compared to cells treated with IR-siRNA after long-term (5 days) knockdown of *SNAI2* in both cell lines ($101 \pm 9 \times 10^3$ versus $355 \pm 14 \times 10^3$ for *SNAI2*-siRNA in PC-3 cells and $20 \pm 1.8 \times 10^3$ versus $63 \pm 3.7 \times 10^3$ for *SNAI2*-siRNA in PC3-16 cells, $p < 0.05$). No significant effect on viability was observed after 72 h of first transfection (data not shown).

SNAI2 knockdown causes a G0/G1 arrest in PC3-16 cells

Potential effects of *SNAI2* siRNA on the cell cycle were investigated by flow cytometry in both cell lines. As is evident in Fig. 4, *SNAI2*-siRNA treatment of the PC3-16 cell line led to an accumulation of most cells in G0/G1 by 72 h after transfection ($84.2 \pm 2.6\%$ in *SNAI2*-siRNA-treated versus $69.6 \pm 0.6\%$ in IR-siRNA-treated cells), whereas little effect was observed in the PC-3 parental line. After a *SNAI2*-siRNA treatment for another 48 h, the G0/G1 arrest in PC3-16 was accentuated (data not shown). Moreover, the amount of apoptotic cells was calculated based on the appearance of cells in “sub-G1,” characteristic of apoptotic cells. The percentage of sub-G1 population changed neither for PC-3 nor for PC3-16 cells. Accordingly, relative activities of caspase-3 and caspase-7 measured by a quantitative luminescence-based assay were only twofold elevated in long-term *SNAI2*-siRNA-treated PC-3 cells, whereas PC3-16 cells did not show any significant changes

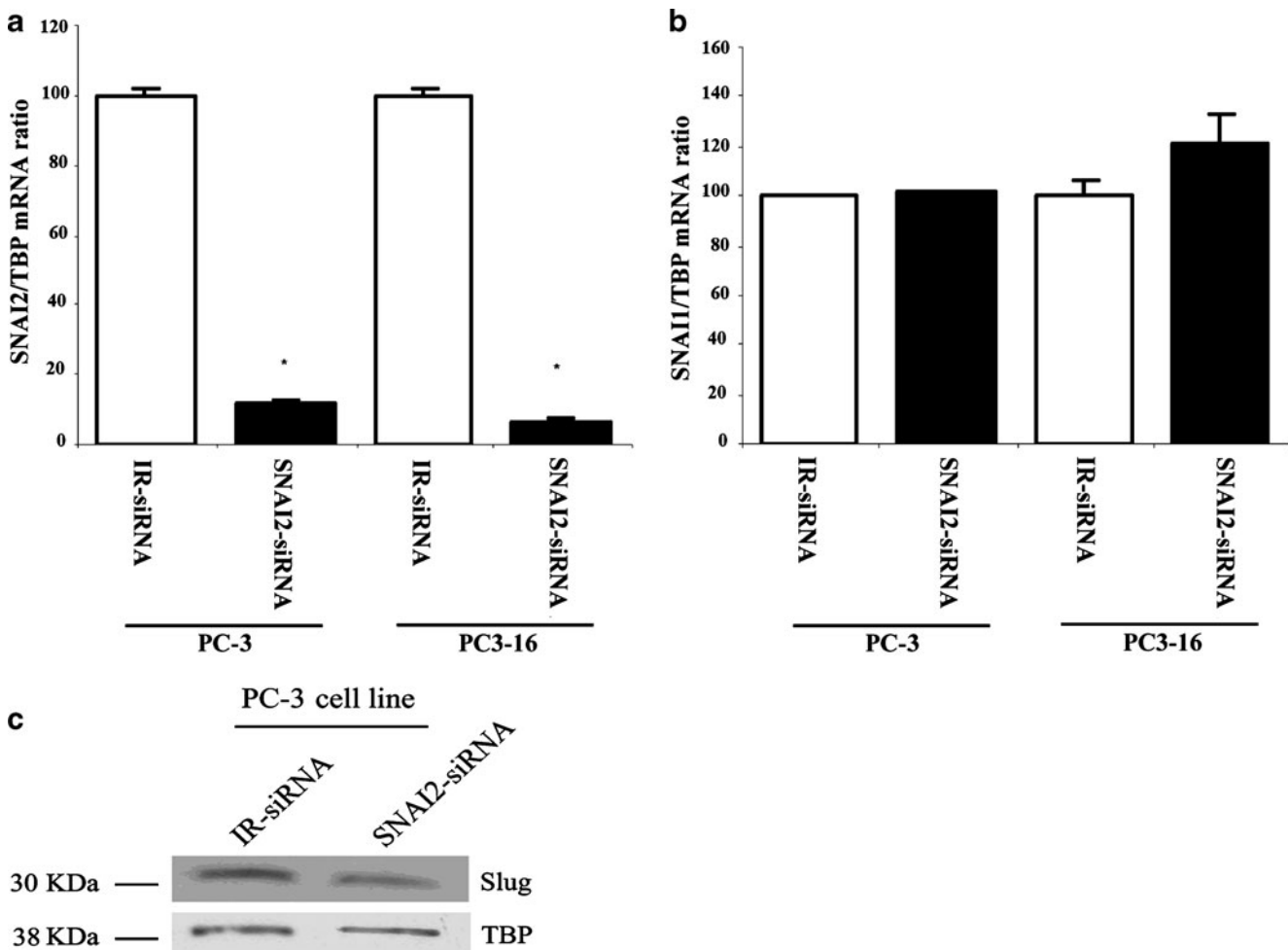


Fig. 2 Effects of SNAI2-siRNA on *SNAI2* and *SNAI1* expression. **a** Downregulation of *SNAI2* mRNA by SNAI2-siRNA in PC-3 and PC3-16 cell lines as determined by quantitative RT-PCR 48 h after transfection. For each cell line, the relative expression of *SNAI2* in IR-siRNA-treated controls was adjusted to 100. **b** Expression of *SNAI1* gene in the two cell lines after SNAI2-siRNA treatment. For each cell

line, the relative expression of *SNAI1* in IR-siRNA-treated controls was adjusted to 100. **c** Effect of SNAI2-siRNA on zinc finger protein SNAI2 levels in PC-3 cells as determined by western blotting, after 72 h. TBP was used as a loading control for western blotting. Asterisks denotes statistically significant differences

in caspase activities (data not shown). Likewise, DAPI staining revealed only rare apoptotic nuclei in attached or detached PC-3 or PC3-16 cells, irrespective of treatment (Supplementary Fig. 1).

SNAI2 knockdown prevents re-adhesion of prostate cancer cells after detachment

Since we noted many floating cells after prolonged treatment with SNAI2 siRNA, we investigated the effect of SNAI2 knockdown on the ability of PC-3 and PC3-16 cells to re-attach to culture plates. For this purpose, siRNA-transfected cells were detached by trypsin and reseeded immediately or after 3 h in suspension into new tissue-culture plates. The cultures were then allowed to grow until mock-treated cells became confluent. SNAI2-siRNA-treated PC-3 and PC3-16 cells did not tolerate detachment from the extracellular matrix

and, immediately after detachment, became unable to re-attach to the tissue-culture plate surface (Fig. 5).

Suppression of SNAI2 expression downregulates expression of integrin $\alpha 6 \beta 4$

To determine a plausible mechanism for the inability of the cells to re-attach after SNAI2 knockdown, we measured the expression of *Integrin $\alpha 6$* (*ITGA4*) and $\beta 4$ (*ITGB6*) mRNA before and after the cells were detached from the extracellular matrix. Expression of *ITGA6* and *ITGB4* decreased in both PC-3 and PC3-16 cell lines (Fig. 6a, b). Determination of integrin $\alpha 6$ protein level by cell surface staining of PC-3 cells confirmed the effect of SNAI2 knockdown on integrin $\alpha 6$ expression (12.1 ± 2.9 versus 7.7 ± 2.4 mean fluorescence intensity for SNAI2-siRNA in PC-3 cells).

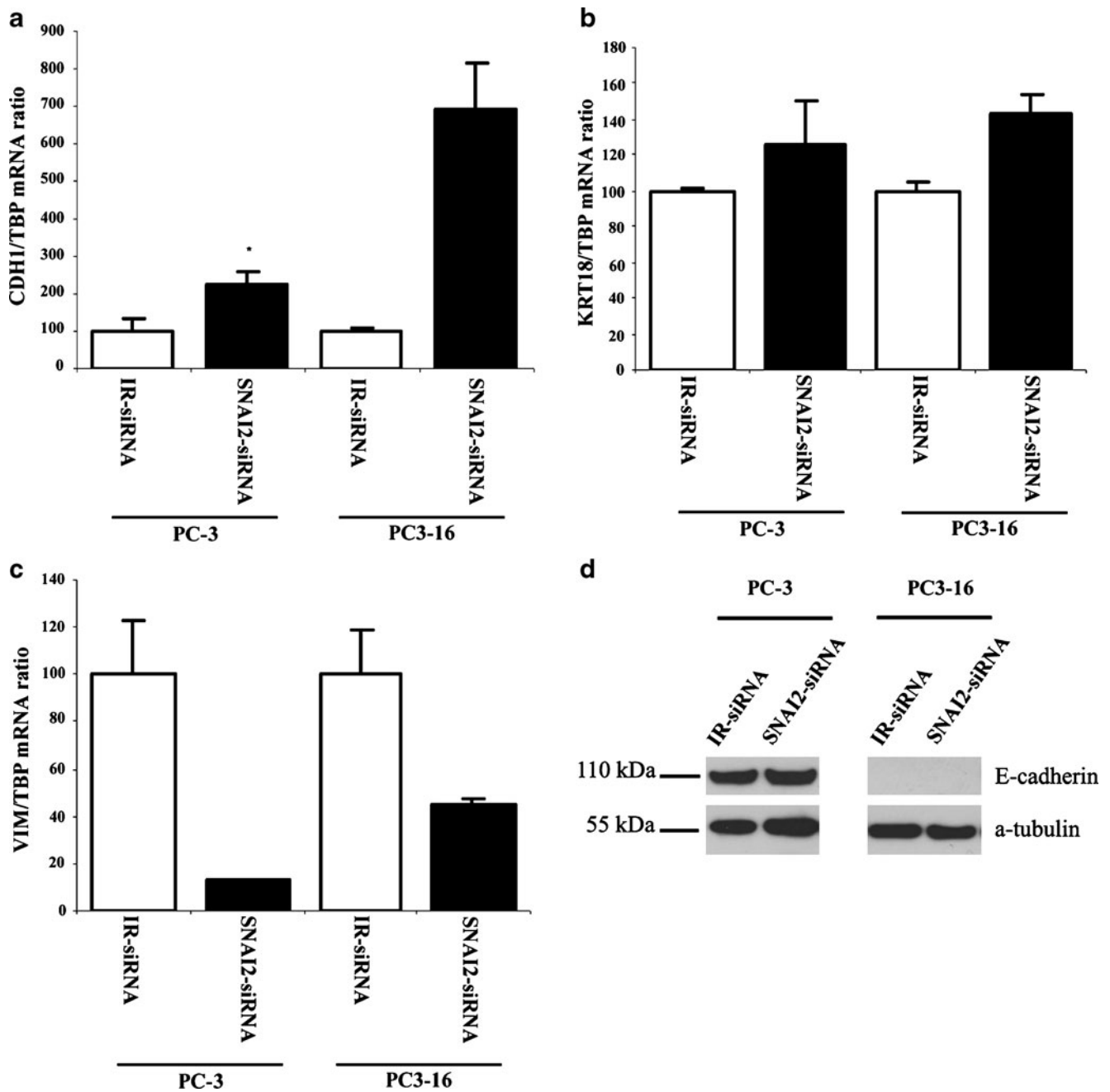


Fig. 3 Expression of different EMT markers after knockdown of SNAI2 expression. **a–c** Relative expression of the genes *CDH1*, *KRT18*, and *VIM* as determined by quantitative RT-PCR. Expression in IR-siRNA-treated controls was adjusted to 100. Values shown

represent the mean \pm SEM. *Asterisk* denotes statistically significant differences. **d** Western blot analysis of E-cadherin relative to α -tubulin expression in PC-3 and PC3-16 cells. Note the general absence of E-cadherin protein in PC3-16 cells

Knockdown of SNAI2 induces a jellyfish-like morphology in PC-3 cells

Microscopic inspection revealed that after SNAI2-siRNA treatment, a significant number of cells (more than 20% in all experiments) became enlarged, flat, and extensively vesiculated. As these features are often indicative of cellular

senescence, we stained the cells for senescence-associated β -galactosidase. However, there was no significant difference between the SNAI2- and IR-siRNA-treated PC-3 cells, with only few cells staining in each group (data not shown). Likewise, staining for γ -tubulin revealed no aberrant mitotic figures (data not shown). Instead, several enlarged cells were multinuclear with indications of failed cytokinesis

Fig. 4 Effect of SNAI2 knock-down on cell cycle distribution in PC-3 and PC3-16 carcinoma cell lines. Cell cycle distribution in PC-3 (**a**) and PC3-16 (**b**) after SNAI2-siRNA treatment. The *upper panels* show the distribution and percentage of cells in the G0/1, S, and G2/M phases, and the *lower panels* show the sub-G1 population of cells as depicted by the FL3 filter of the FACS instrument

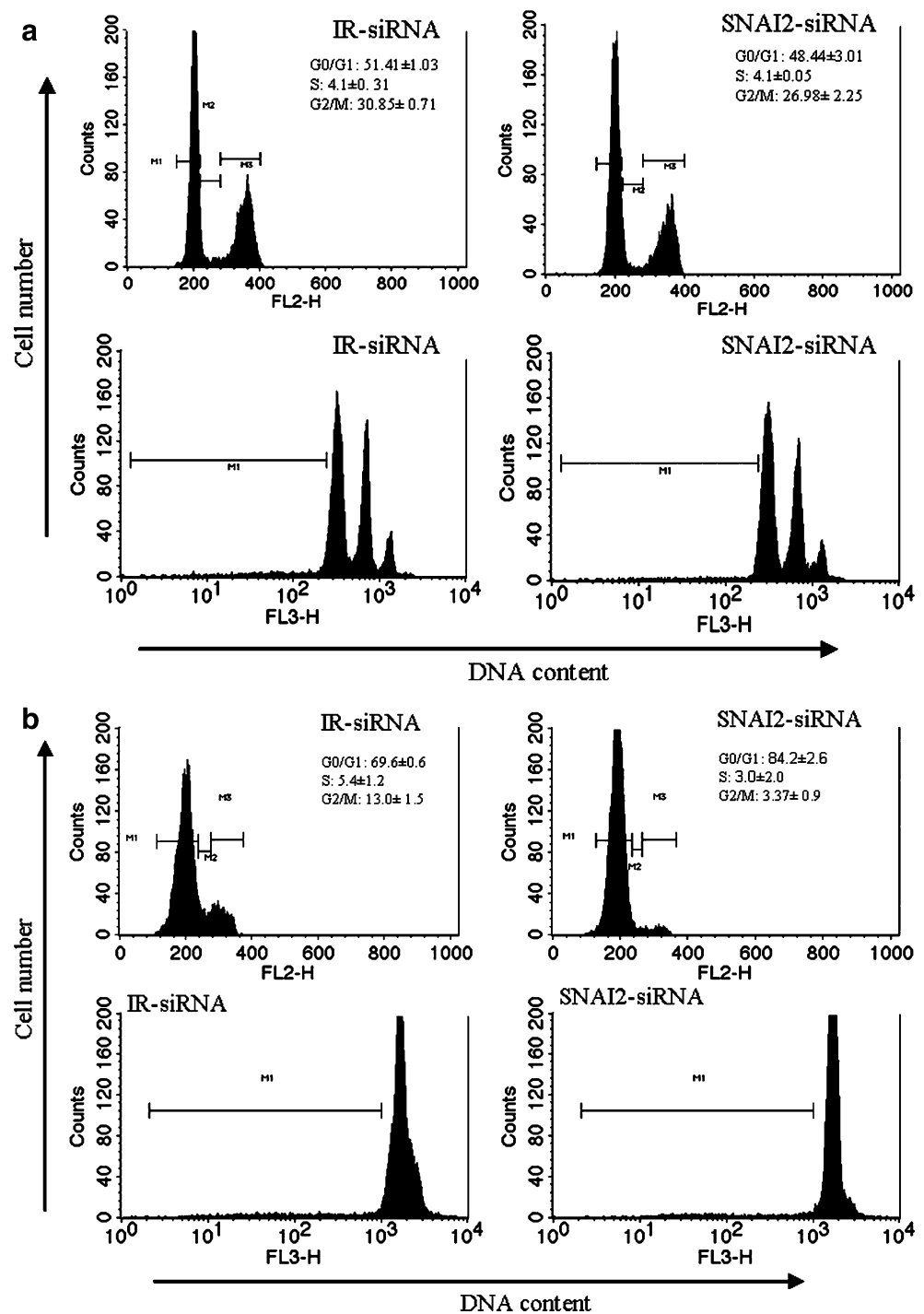


(Fig. 7). Accordingly, immunocytochemistry for α -tubulin and β -actin showed that the cytoskeleton had rearranged dramatically in many SNAI2-siRNA-treated PC-3 cells (Fig. 7). The microtubule cytoskeleton specifically rearranged into O- and C-shaped rings, whereas the margin of these cells displayed condensed patches of α -tubulin. In the ring-like structures, microtubule and actin cytoskeletons had tangled up and lost their ordered organization.

Suppression of SNAI2 expression abolishes invasiveness of PC-3 and PC3-16 cells

Finally, to determine the effect of SNAI2 knockdown on invasiveness of PC-3 and PC3-16 cells, a Matrigel invasion assay was performed. Treatment of PC-3 cells with SNAI2-siRNA caused a significant ($p < 0.05$) decrease in the number of cells capable of migration through the matrix

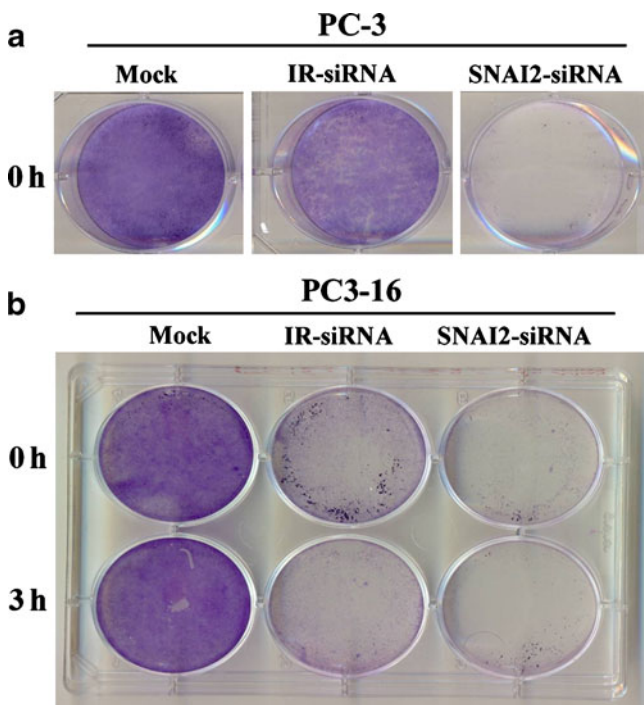


Fig. 5 Effect of SNAI2 knockdown on cell re-attachment. Cells treated with siRNA for 2 days were detached from the ECM and kept in suspension for up to 3 h before reseeding. After the mock-treated cells became confluent, cells were fixed and stained with Giemsa. PC-3 cells, treated with different siRNAs, cultivated in standard tissue-culture plates, immediately after suspension in a bacterial plate (a). PC3-16 cells, treated with IR-siRNA or SNAI2-siRNA, suspended for 0 (top row) and 3 h (bottom row) in a bacterial plate and then cultivated in standard tissue-culture plates (b)

(Fig. 8) compared to cells treated with IR-siRNA. In PC3-16, the decrease was even more pronounced, and only a minimal number of cells penetrated the matrix at all (data not shown).

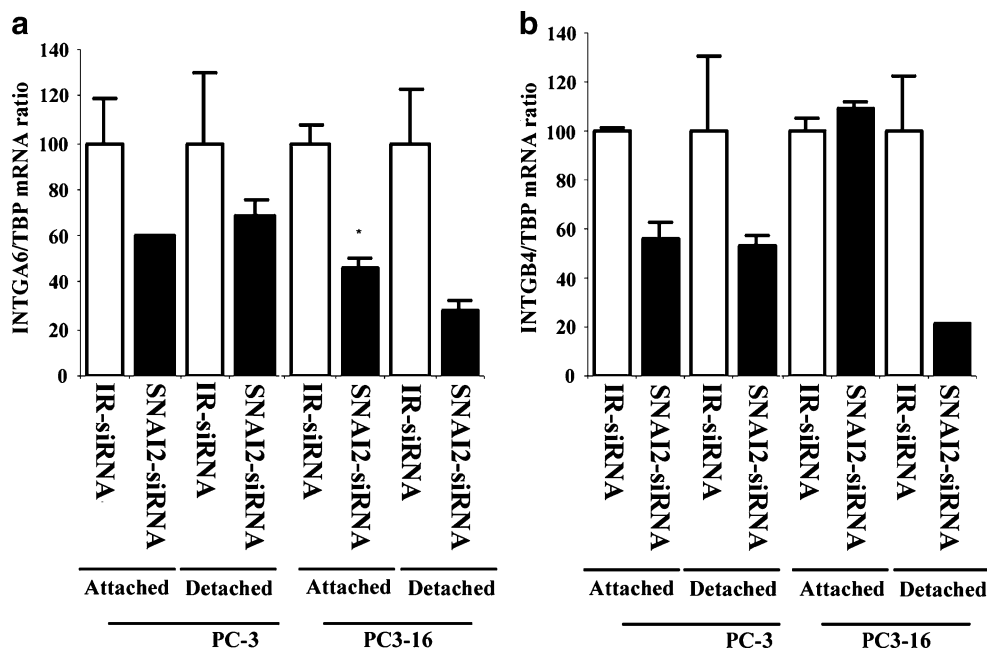
Discussion

The zinc finger proteins SNAI1 (Snail) and SNAI2 (Slug) are best known as inducers of EMT, but appear to exert additional functions during normal development as well as during cancer progression [1]. In this first study of SNAI2 in prostate cancer cells, we have indeed obtained evidence for both kinds of function.

By qRT-PCR, *SNAI2* expression was predominantly observed in the PC-3 line and its derivatives, especially the PC3-16 subline that exhibits a more mesenchymal phenotype. This finding suggests that the involvement of *SNAI2* can differ even between tumors of the same type, such as metastatic prostate cancers. Intriguingly, normal prostate epithelial cells too expressed *SNAI2* mRNA during growth in culture. These cells are grown in media with multiple growth supplements including EGF to support viability and the proliferative capacity of these cells. Such growth factors have been found to lead to the upregulation of Snail genes in various cellular contexts [1]. Evidently, the effect of growth factors on the expression of Snail genes in normal and cancerous prostate cancer cells deserves a closer investigation in future work.

Downregulation of SNAI2 by siRNA in PC-3 cell lines increased the expression of the mRNA for epithelial markers such as E-cadherin and cytokeratin 18. As loss of

Fig. 6 Expression of *INTGA6* and *INTGB4* after SNAI2 knockdown. Expression of *INTGA6* (a) and *INTGB4* (b) mRNA in PC-3 and PC3-16 cells measured before and after the siRNA-treated cells were detached from the extracellular matrix, according to real-time PCR with *TBP* as a control. For each cell line, the relative expression of the genes in IR-siRNA-treated controls was adjusted to 100. Values shown represent the mean ± SEM. Asterisk denotes statistically significant differences



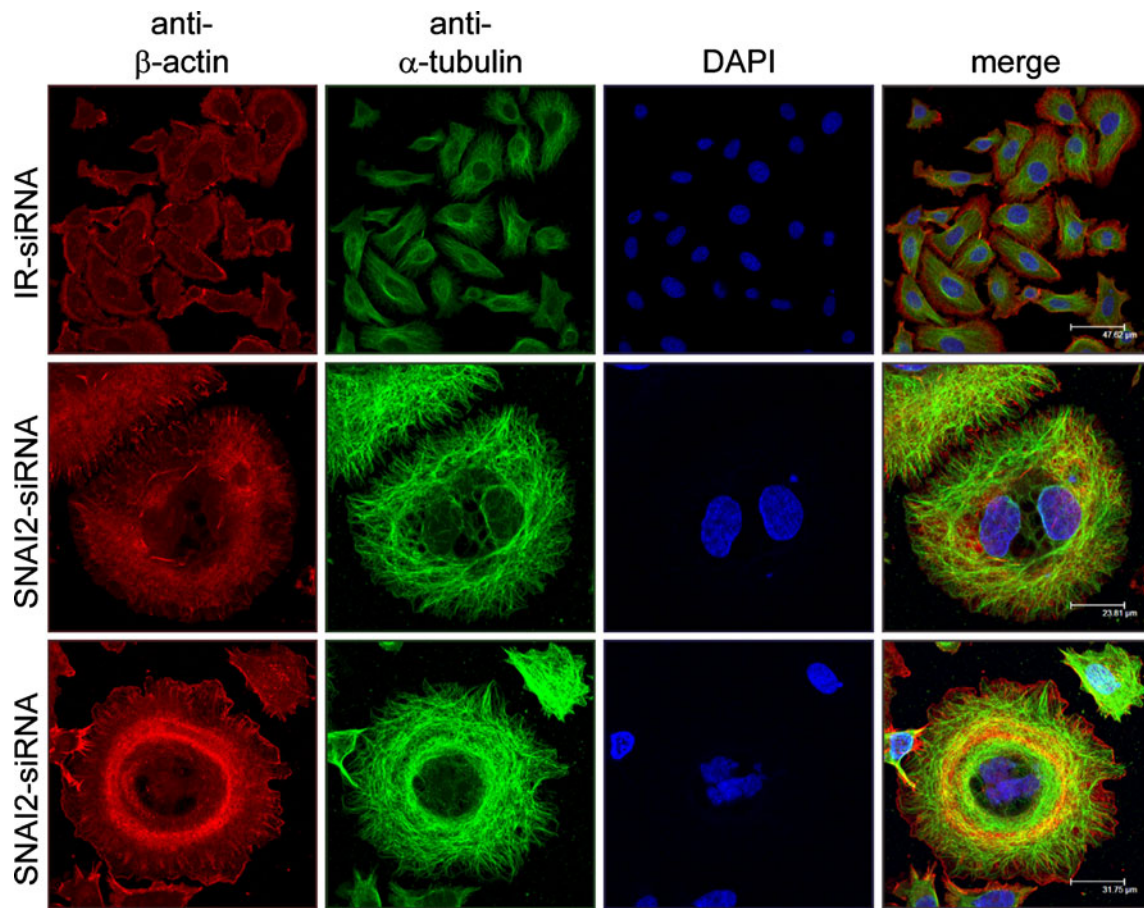


Fig. 7 Rearrangement of cytoskeletons in SNAI2-treated PC-3 cells. Microtubules (*green*) and actin (*red*) were detected using α -tubulin and actin specific antibodies. DNA was visualized by 4,6-diamidino-2-phenylindole (*DAPI*)

E-cadherin is considered a hallmark of EMT [18], this finding is consistent with a function of SNAI2 in EMT induction. Of note, effects of SNAI2 on E-cadherin expression have been observed in most cancer cells, but

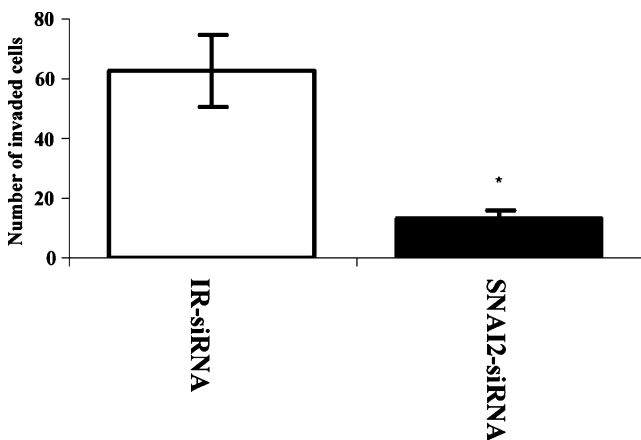


Fig. 8 The effect of SNAI2 knockdown on invasiveness of the PC-3 cell line. Number of PC-3 cells having invaded the ECM substrate after siRNA treatment as indicated. The data shown are representative for three independent experiments. Values shown represent the mean \pm SEM. Asterisk indicates statistically significant differences

not all. For instance, SNAI2 repressed E-cadherin in breast, lung, and esophageal carcinoma cell lines [7] but not in NBT-II rat bladder carcinoma cells [8]. Our data predict that SNAI2 could be a repressor of E-cadherin in those metastatic prostate cancers that express it at sufficient levels. Intriguingly, PC3-16 cells, in contrast to the parental line, did not express E-cadherin protein, despite the presence of residual mRNA. Apparently, this loss is one change that has occurred during the in vivo selection for a more metastatic variant of PC3. In addition, according to our data, SNAI2 also influences other characteristics of EMT in prostate cancer cells, including upregulation of mesenchymal markers such as vimentin and enhanced invasiveness [19], which were reversed by *SNAI2* knockdown.

Altered adhesion to the extracellular matrix is another typical property of invasive tumor cells. It is therefore interesting that we observed a rather dramatic effect of SNAI2 suppression on the ability of PC-3 cell lines to reattach to culture plates. At least part of this effect could be mediated by reduced expression of integrins $\alpha 6$ and $\beta 4$, which together form an adhesion receptor for laminins of the ECM [20]. By means of their association with F-actin on one hand and the extracellular matrix on the other hand,

integrins can harness traction forces generated by actomyosin contraction [21], which are used to move cells to forward direction on a rigid matrix [22]. Downregulation of integrins as a consequence of *SNAI2* knockdown could therefore account not only for diminished cell adhesion but also decreased ability to invade a matrigel substrate. The promoters of the genes encoding integrins $\alpha 3$, $\alpha 6$, and $\beta 4$ all contain potential E-boxes, suggesting that they may constitute direct targets of *SNAI* zinc finger proteins [23–25]. Accordingly, it was recently reported that overexpression of *SNAI2* in keratinocytes resulted in the altered expression of several integrins, including the $\alpha 3$, $\beta 1$, and $\beta 4$ proteins [26]. Taken together, that study and the present one indicate that the regulation of integrins by Snail factors in normal and cancerous cells ought to be investigated in more detail.

Actin filament and microtubule networks cooperate functionally during a wide variety of cellular processes, including cell migration and vesicular transport [27]. Our data demonstrate that *SNAI2* knockdown caused a pronounced cytoskeletal rearrangement, especially dramatic in PC-3 cells that appeared to disturb the functional cooperation between the microtubule and actin cytoskeletons, resulting in grossly enlarged cells with multiple nuclei in some cases. Multinucleation in particular might ensue, since the proper placement of the cleavage plane (the site of cytokinesis) also requires interactions between microtubules and the cortical actin cytoskeleton. This finding indicates that the function of *SNAI2* on prostate cancer cells may extend—directly or indirectly—beyond cytokeratin and integrin expression to the broader organization of the various components of the cytoskeleton. A further phenomenon supporting this idea is that *SNAI2*-siRNA-treated PC-3 cells became vesiculated, indicating likewise that coordinated microtubule- and actin-based transport was defective in these cells.

SNAI2 knockdown had similar effects on EMT markers, integrin expression, and invasiveness in the PC-3 parental cell line and its more metastatic derivative PC3-16, which harbors various additional chromosomal changes [12] and expresses *SNAI2* more strongly (Fig. 1). The above effect of *SNAI2* knockdown on cell morphology was more pronounced in the parental line. In contrast, our data demonstrate that *SNAI2* downregulation caused a prominent G0/G1 arrest especially in PC3-16 cells. This finding is not entirely unprecedented. *SNAI2* siRNA treatment increased the capacity of fotemustine to elicit cell death and induced p21WAF1 upregulation in melanoma cells, resulting in cell cycle arrest [28]. Likewise, expression of cyclins D2 and G2 was diminished in the epidermis of *Snai2* knockout mice, associated with decreased levels of proliferation [29]. In other cell types, *SNAI2* has been found to act as a survival factor in addition to or even

before inducing EMT [30], whereas we observed only a slight effect of *SNAI2* knockdown on apoptosis in the PC-3 cell lines. This evidently does not contradict the findings in other cell types, particularly normal cells, because survival of prostate cancer cells may be ensured by many other factors altered during carcinogenesis.

In summary, to our knowledge, these results show for the first time that zinc finger protein *SNAI2* may have unexpectedly diverse functions in prostate cancer cells. As shown here, *SNAI2* appears to affect classical EMT markers, but also to possess an important additional function in the organization of the cytoskeleton and cell adhesion molecules. Through these functions, *SNAI2* may impinge on invasivity and cell proliferation, and in some cells, it may even directly influence the cell cycle. Our findings call for further studies to elucidate the precise molecular mechanisms by which *Slug* affects cell shape and adhesion.

Acknowledgments We thank Christiane Hader and Dr. Parvaneh Nikpour for valuable assistance in several experiments and helpful suggestions.

References

- Barrallo-Gimeno A, Nieto MA. The snail genes as inducers of cell movement and survival: implications in development and cancer. *Development*. 2005;132:3151–61.
- Baum B, Settleman J, Quinlan MP. Transitions between epithelial and mesenchymal states in development and disease. *Semin Cell Dev Biol*. 2008;19:294–308.
- Hemavathy K, Guru SC, Harris J, Chen JD, Ip YT. Human slug is a repressor that localizes to sites of active transcription. *Mol Cell Biol*. 2000;20:5087–95.
- Alves CC, Carneiro F, Hoefler H, Becker KF. Role of the epithelial-mesenchymal transition regulator slug in primary human cancers. *Front Biosci*. 2009;14:3035–50.
- Perez-Caro M, Bermejo-Rodriguez C, Gonzalez-Herrero I, Sanchez-Beato M, Piris MA, Sanchez-Garcia I. Transcriptomal profiling of the cellular response to DNA damage mediated by slug (*snai2*). *Brit J Cancer*. 2008;98:480–8.
- Bolos V, Peinado H, Perez-Moreno MA, Fraga MF, Esteller M, Cano A. The transcription factor slug represses e-cadherin expression and induces epithelial to mesenchymal transitions: a comparison with snail and e47 repressors. *J Cell Sci*. 2003;116:499–511.
- Hajra KM, Chen DY, Fearon ER. The slug zinc-finger protein represses e-cadherin in breast cancer. *Cancer Res*. 2002;62:1613–18.
- Savagner P, Yamada KM, Thiery JP. The zinc-finger protein slug causes desmosome dissociation, an initial and necessary step for growth factor-induced epithelial-mesenchymal transition. *J Cell Biol*. 1997;137:1403–19.
- Tripathi MK, Misra S, Chaudhuri G. Negative regulation of the expressions of cytokeratins 8 and 19 by slug repressor protein in human breast cells. *Biochem Biophys Res Commun*. 2005;329:508–15.
- Perez-Mancera PA, Gonzalez-Herrero I, Maclean K, Turner AM, Yip MY, Sanchez-Martin M, et al. Slug (*Snai2*) overexpression in embryonic development. *Cytogenet Genome Res*. 2006;114:24–9.

11. Perez-Mancera PA, Gonzalez-Herrero I, Perez-Caro M, Gutierrez-Cianca N, Flores T, Gutierrez-Adan A, et al. Slug in cancer development. *Oncogene*. 2005;24:3073–82.
12. Lensch R, Gotz C, Andres C, Bex A, Lehmann J, Zwergel T, et al. Comprehensive genotypic analysis of human prostate cancer cell lines and sublines derived from metastases after orthotopic implantation in nude mice. *Int J Oncol*. 2002;21:695–706.
13. Wlazlinski A, Engers R, Hoffmann MJ, Hader C, Jung V, Muller M, et al. Downregulation of several fibulin genes in prostate cancer. *Prostate*. 2007;67:1770–80.
14. Jafarnejad SM, Mowla SJ, Matin MM. Knocking-down the expression of nucleostemin significantly decreases rate of proliferation of rat bone marrow stromal stem cells in an apparently p53-independent manner. *Cell Prolif*. 2008;41:28–35.
15. Dimri GP, Lee X, Basile G, Acosta M, Scott G, Roskelley C, et al. A biomarker that identifies senescent human cells in culture and in aging skin in vivo. *Proc Natl Acad Sci USA*. 1995;92:9363–7.
16. Janssen K, Pohlmann S, Janicke RU, Schulze-Osthoff K, Fischer U. Apaf-1 and caspase-9 deficiency prevents apoptosis in a bax-controlled pathway and promotes clonogenic survival during paclitaxel treatment. *Blood*. 2007;110:3662–72.
17. Engers R, Springer E, Michiels F, Collard JG, Gabbert HE. Rac affects invasion of human renal cell carcinomas by up-regulating tissue inhibitor of metalloproteinases (Timp)-1 and Timp-2 expression. *J Biol Chem*. 2001;276:41889–97.
18. Guarino M, Rubino B, Ballabio G. The role of epithelial-mesenchymal transition in cancer pathology. *Pathology*. 2007;39:305–18.
19. Lee JM, Dedhar S, Kalluri R, Thompson EW. The epithelial-mesenchymal transition: new insights in signaling, development, and disease. *J Cell Biol*. 2006;172:973–81.
20. Pouliot N, Connolly LM, Moritz RL, Simpson RJ, Burgess AW. Colon cancer cells adhesion and spreading on autocrine laminin-10 is mediated by multiple integrin receptors and modulated by egf receptor stimulation. *Exp Cell Res*. 2000;261:360–71.
21. Ridley AJ, Schwartz MA, Burridge K, Firtel RA, Ginsberg MH, Borisy G, et al. Cell migration: integrating signals from front to back. *Science*. 2003;302:1704–9.
22. Lipscomb EA, Mercurio AM. Mobilization and activation of a signaling competent alpha6beta4 integrin underlies its contribution to carcinoma progression. *Cancer Metastasis Rev*. 2005;24:413–23.
23. Kato T, Katabami K, Takatsuki H, Han SA, Takeuchi K, Irimura T, et al. Characterization of the promoter for the mouse alpha 3 integrin gene. *Eur J Biochem*. 2002;269:4524–32.
24. Lin CS, Chen Y, Huynh T, Kramer R. Identification of the human alpha6 integrin gene promoter. *DNA Cell Biol*. 1997;16:929–37.
25. Takaoka AS, Yamada T, Gotoh M, Kanai Y, Imai K, Hirohashi S. Cloning and characterization of the human beta4-integrin gene promoter and enhancers. *J Biol Chem*. 1998;273:33848–55.
26. Turner FE, Broad S, Khanim FL, Jeanes A, Talma S, Hughes S, et al. Slug regulates integrin expression and cell proliferation in human epidermal keratinocytes. *J Biol Chem*. 2006;281:21321–31.
27. Goode BL, Drubin DG, Barnes G. Functional cooperation between the microtubule and actin cytoskeletons. *Curr Opin Cell Biol*. 2000;12:63–71.
28. Vannini I, Bonafe M, Tesei A, Rosetti M, Fabbri F, Storci G, et al. Short interfering rna directed against the slug gene increases cell death induction in human melanoma cell lines exposed to cisplatin and fotemustine. *Cell Oncol*. 2007;29:279–87.
29. Newkirk KM, MacKenzie DA, Bakaletz AP, Hudson LG, Kusewitt DF. Microarray analysis demonstrates a role for slug in epidermal homeostasis. *J Invest Dermatol*. 2008;128:361–9.
30. Robson EJ, Khaled WT, Abell K, Watson CJ. Epithelial-to-mesenchymal transition confers resistance to apoptosis in three murine mammary epithelial cell lines. *Differentiation*. 2006;74:254–64.